December, 2011

Observations of the vertical ion drift in the equatorial ionosphere during the solar minimum period of 2009

R. A. Stoneback
R. A. Heelis
A. G. Burrell
W. R. Coley
Bela G. Fejer, *Utah State University*, et al.

Observations of quiet time vertical ion drift in the equatorial ionosphere during the solar minimum period of 2009

R. A. Stoneback,[1] R. A. Heelis,[1] A. G. Burrell,[1] W. R. Coley,[1] B. G. Fejer,[2] and E. Pacheco[2]

Received 31 March 2011; revised 25 October 2011; accepted 26 October 2011; published 29 December 2011.

[1] The extended solar minimum conditions in 2008 and 2009 presented an opportunity to investigate the ionosphere at lower solar activity levels than previously observed. The Coupled Ion Neutral Dynamics Investigation (CINDI) Ion Velocity Meter (IVM) instrument onboard the Communication/Navigation Outage Forecasting System is used to construct the median meridional (vertical) ion drifts, ion densities, and O+ concentrations during periods of low geomagnetic activity for four characteristic seasons each year spanning late 2008 to 2010. The presence of a large semidiurnal component in the ion drift variation at the equator produced significant differences from typical ionospheric conditions. Instead of upward drifts during the day and downward drifts at night, downward drifts in the afternoon and upward drifts near midnight are observed. This semidiurnal component is present in all seasons though it is strongest during the solstice seasons. It is shown that upward drifts at night correspond to regions with a high occurrence of postmidnight irregularities during the December 2008 and June 2009 solstices. A comparison with vertical ion drifts observed by the Jicamarca Radio Observatory supports the methodology used to extract meridional drifts from the IVM.

Citation: Stoneback, R. A., R. A. Heelis, A. G. Burrell, W. R. Coley, B. G. Fejer, and E. Pacheco (2011), Observations of quiet time vertical ion drift in the equatorial ionosphere during the solar minimum period of 2009, *J. Geophys. Res.*, *116*, A12327, doi:10.1029/2011JA016712.

1. Introduction

[2] The ion drift velocity in the equatorial ionosphere is one of the most important parameters affecting the distribution of ionization and the appearance and evolution of ionospheric irregularities in the region. In the equatorial region extensive observations of the vertical ion drift have been made from the ground [*Fejer et al.*, 1991] and from satellites [*Kil et al.*, 2009]. Such observations have been organized by season and solar activity level and have been used to produce an empirical description [*Scherliess and Fejer*, 1999] that is commonly used to represent the average behavior of the ionosphere in computational models [*Huba et al.*, 2000].

[3] All these observations show that the most dramatic variations in the drift velocity with respect to local time are due to the influence of *E* region migrating and nonmigrating tides on the electric field [*Millward et al.*, 2001]. Winds in the *F* region have also been invoked to explain drift features that have shorter durations in local time, such as the prereversal enhancement [*Eccles*, 1998] and the predawn decrease [*Pacheco et al.*, 2010].

[4] Seasonal and longitude variations in the vertical ion drift are also significant near the equator. These variations may be attributed to longitude variations in the tropospheric nonmigrating tides [*Hagan et al.*, 2007]. The offset between the geographic and geomagnetic equators, which places the flux tube feet at different latitudes, may also contribute to these variations. Recent studies have also demonstrated that sudden stratospheric warming events can alter drifts at the equator [*Anderson and Araujo-Pradere*, 2010; *Chau et al.*, 2009; *Rodrigues et al.*, 2011]. A slowdown or reversal in the polar wind in the northern winter hemisphere drives an increase in stratospheric temperature. This disturbance propagates to midlatitudes and low latitudes, perturbing the meridional ion drift. Finally, the equatorial vertical ion drift is influenced by solar and magnetic activity. The effects of magnetic activity are manifested in electric fields of magnetospheric origin that penetrate from high to low latitudes [*Peymirat et al.*, 2000] and in modifications to the low-latitude dynamo wind system produced by frictional heating and particle heating at high latitudes [*Blanc and Richmond*, 1980]. The effects of solar activity have been well documented in ground-based observations at the magnetic equator [*Fejer et al.*, 1991], although the processes responsible for the observed changes in the local time variation of the vertical ion drift are not well described. Changes in the ion density distribution also affect the ion drag force on neutral particles as well as the ionospheric conductivity. Despite the obvious

[1]Physics Department, Hanson Center for Space Sciences, University of Texas at Dallas, Richardson, Texas, USA.
[2]Center of Atmospheric and Space Sciences, Utah State University, Logan, Utah, USA.

0148-0227/11/2011JA016712

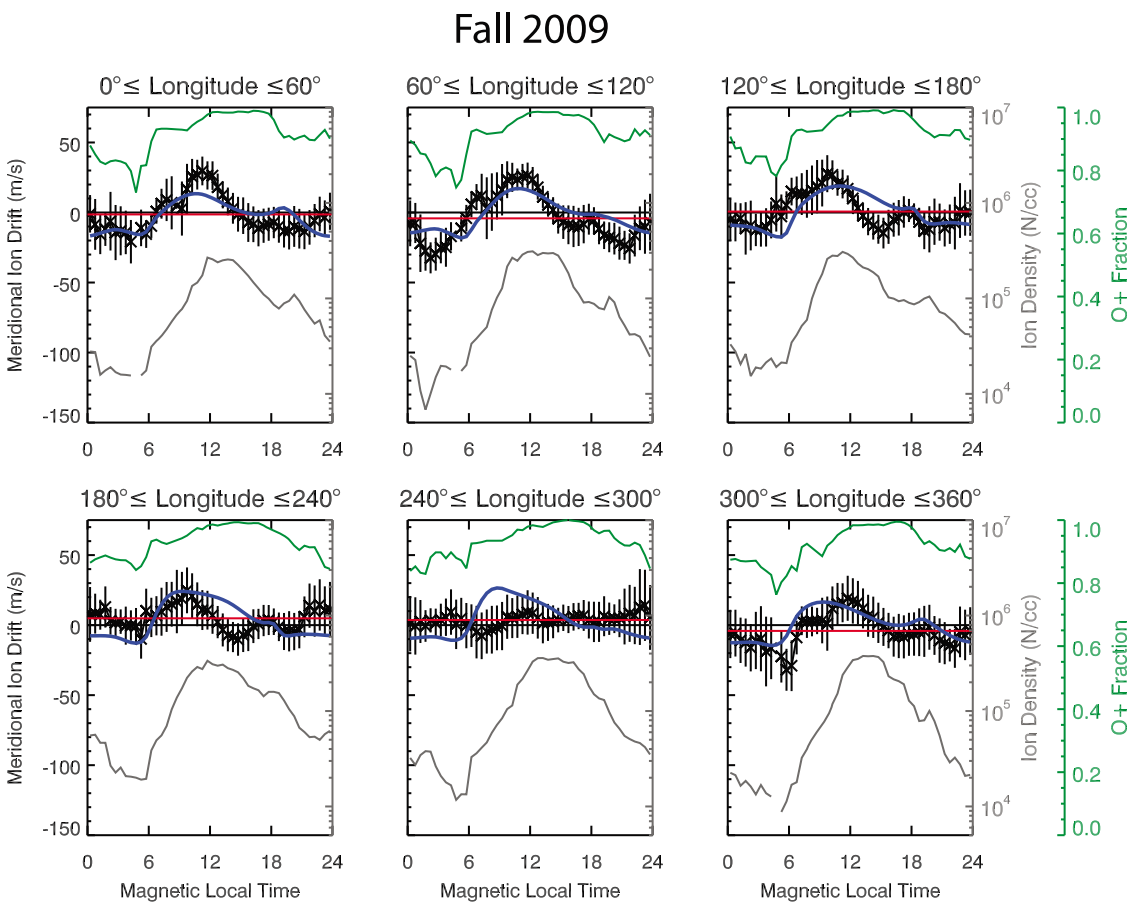

Figure 1. Magnetic local time variations in the meridional ion drift, total ion concentration, and O+ fraction for different longitude regions during fall 2009. Drifts from the Scherliess-Fejer model are included in blue.

importance of these parameters for the equatorial dynamo, observations are currently unavailable.

[5] This paper reports the local time variations in meridional (vertical) ion drifts in the equatorial *F* region for altitudes between 400 and 550 km and periods of low geomagnetic activity during the prolonged solar minimum period covering 2008–2009 and into 2010. Data obtained from the Coupled Ion Neutral Dynamics Investigation (CINDI) that flies aboard the Communication/Navigation Outage Forecast System (C/NOFS) satellite describes the seasonal changes in the local time variation of the vertical ion drift at different longitudes.

2. Observations

[6] The CINDI instrumentation includes a planar retarding potential analyzer and a planar ion drift meter that together provide a measure of the total ion concentration and the vector ion drift in the satellite reference frame [*Heelis and Hanson*, 1998]. These instruments fly onboard the C/NOFS satellite in a 13° inclination orbit with perigee near 400 km and apogee near 860 km. The satellite was launched in April 2008 during an extended solar minimum period when the 10.7 cm solar radio flux (F10.7) remained below 80 $\times$ 10^{-22} Wm^{-2} Hz^{-1} for the following 24 months. Low ionospheric densities due to the extended solar minimum along with operating characteristics of CINDI restricted drift measurements to altitudes near perigee, limiting the local time coverage of a given orbit. However, the precession of the orbit plane allows all local times and longitudes to be sampled below 550 km altitude in 67 d, thus the local time, longitude and seasonal characteristics of the ion drifts can be described. This study considers measurements of the equatorial meridional (vertical) ion drift taken during 2009 and 2010 and describes this behavior for four characteristic seasons each year.

[7] Measurements of the ion drift and total ion concentration were made from the three axis stabilized satellite every half second with the reference axes maintained approximately in the direction of the satellite motion, along the local vertical in the orbit plane and along the local horizontal perpendicular to the orbit plane. Measurements of the ambient ion drift require that the spacecraft velocity be removed with very high accuracy. Thus the inertial attitude of the spacecraft and any offsets between the reference axes of the attitude determination system and the instrument measurement system must be accurately specified. A significant examination of the long-term trends in the measured ion drifts is required to determine these offsets. In the altitude region between 400 km and 550 km the ion drift perpendicular to the magnetic field and electric field are related by the expressions $\mathbf{E} = -\mathbf{V} \times \mathbf{B}$ and $\nabla \times \mathbf{E} = 0$. Thus offsets in the ion drift

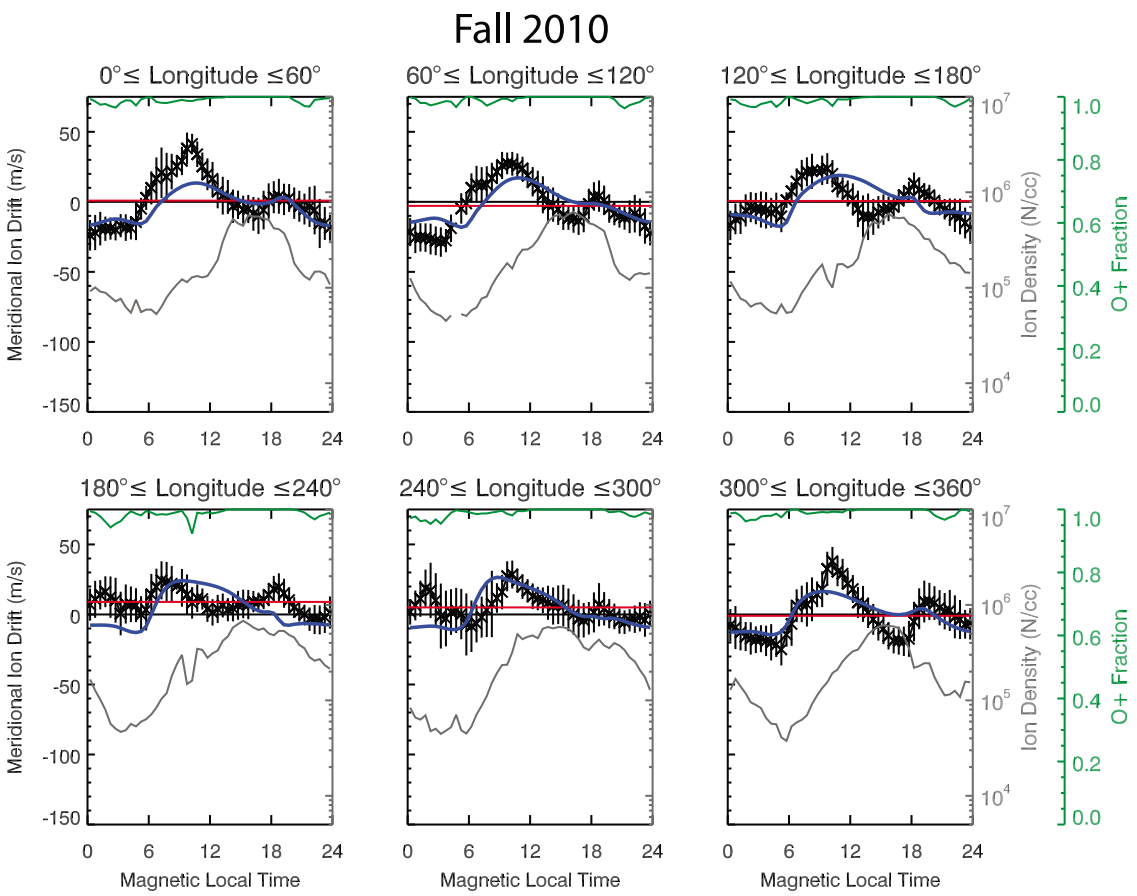

Figure 2. Magnetic local time variations in the meridional ion drift, total ion concentration, and O+ fraction for different longitude regions during fall 2010. Drifts from the Scherliess-Fejer model are included in blue.

components can be determined by requiring that the longitude and local time average of the meridional ion drift be zero. Offsets in the local vertical and local horizontal components are isolated based on the symmetry of each component in the meridional direction across the magnetic equator. The local horizontal points generally northward, contributing positively to the meridional direction in the northern hemisphere and negatively in the southern. The local vertical is generally radial, contributing positively to the meridional direction in both hemispheres. By computing the mean meridional drift over all local times and longitudes as a function of magnetic latitude both the symmetric and antisymmetric offset terms can be identified and removed. The offset for each measurement direction is a slowly varying constant, changing by less than 1 m s^{-1} d^{-1}. Corrected drifts are produced in the spacecraft frame by subtracting the determined offsets from measurements. The corrected meridional ion drift can then be evaluated as a function of local time, longitude and season. Details on the offset calculation and results will follow in a future publication.

[8] We have divided the year into approximately 2 month periods (67 d) representing the northern hemispheric seasons: fall (September, October), spring (March, April), winter (December, January) and summer (June, July). A 2 month period has been chosen so that all local times are sampled equally as perigee precesses in local time. Two precession periods (134 d) are too long for three nonoverlapping seasons in a year. For each of the 2 monthlong seasons we divide the globe into 60 degree longitude sectors and 30 min local time sectors. In each bin the median value and the average absolute deviation from the median is computed if the bin contains more than 300 samples. A running centered 400 km average ion density along the satellite track is established and used to exclude data points where the normalized deviation from the average is large, $\Delta N/N > 10\%$, limiting the influence of plasma irregularities upon the presented averages. The 3 h Kp index is required to be less than or equal to 3 for the previous 24 h, restricting data to periods of low geomagnetic activity.

[9] A lower limit for the O+ concentration of 3×10^3 cm^{-3} is maintained that ensures a sufficient signal to the drift meter detectors for each data point. A first-order correction has also been applied when asymmetric suppression of photoemission from internal surfaces in the detectors can create an erroneous signal. Details relating to the refraction of light in the Earth's atmosphere near the dawn terminator and the resultant changes in solar intensity have not been determined, thus drift measurements near the dawn terminator are excluded. The significance of photoemission is seasonally dependent, with minima during equinox and maxima during the solstices because of the satellite's orientation with respect to the Sun. The effect of photoemission is also ion density dependent,

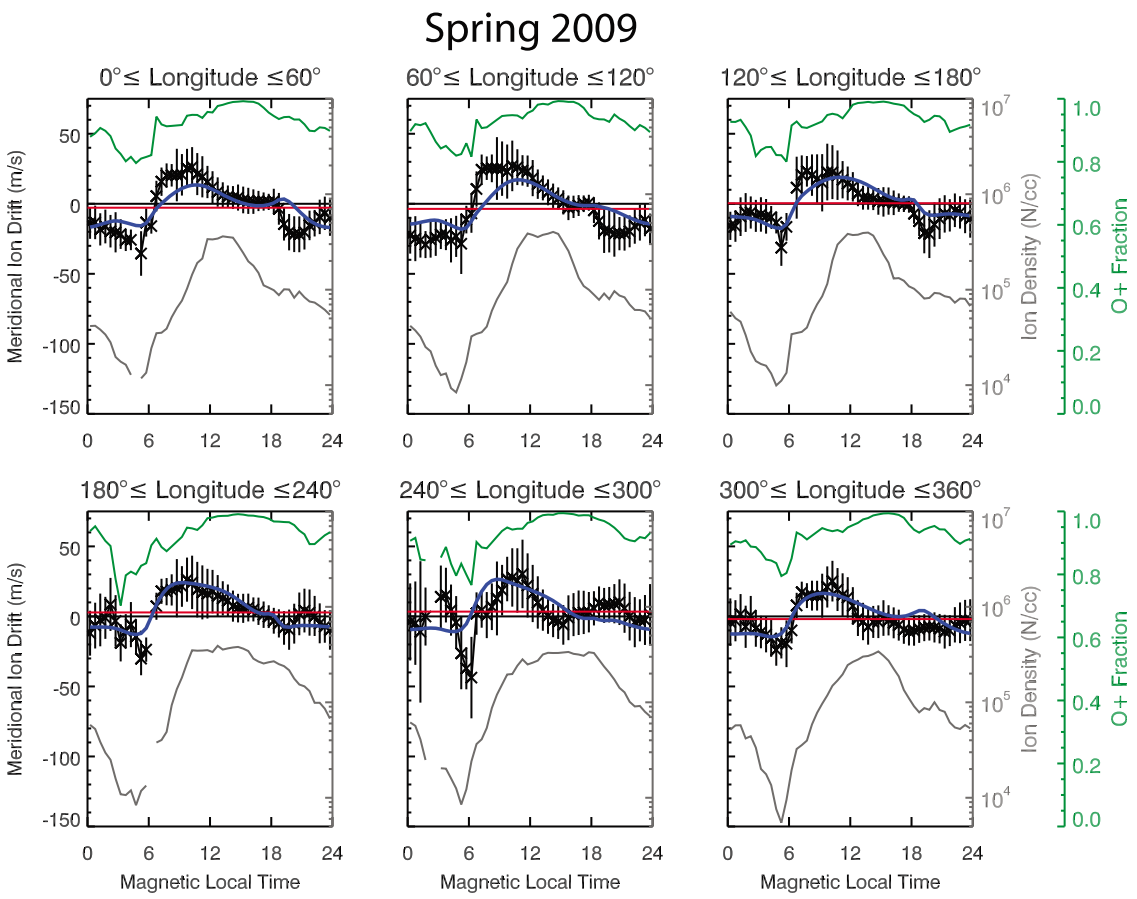

Figure 3. Magnetic local time variations in the meridional ion drift, total ion concentration, and O+ fraction for different longitude regions during spring 2009. Drifts from the Scherliess-Fejer model are included in blue.

larger errors are observed with lower O+ densities. Photoemission generally occurs within the IDM between 05:00 and 10:00 magnetic local time (MLT), thus reported values during this time have additional uncertainty that decreases dramatically for densities larger than 3×10^4 cm^{-3}. A filter has also been applied to remove erroneous measurements that occur for particular solar incidence angles with respect to the spacecraft, generally found between 08:00–09:00 local time. Thus apparent local time variations over this short time period should be viewed with some caution.

[10] Restrictions on the O+ concentration largely limit measurements to altitudes below 550 km thus the local time coverage of the satellite is determined by perigee. As perigee moves through 24 h of local time in 67 d F10.7 can change significantly. Since perigee only covers a given local time once in a season and measurements are restricted to altitudes near perigee, variations in F10.7 can lead to ionospheric densities that are not well represented by averages. If measurements are restricted to within 10° of the magnetic equator, the local time coverage of any given pass is further restricted. Thus measurements over the entire latitude range of C/NOFS are presented, however, this expanded latitude range reduces the direct correlation of meridional drifts and densities.

[11] The measured ion drift is resolved parallel and perpendicular to the magnetic field using the International Geomagnetic Reference Field. The perpendicular component of the ion drift is then resolved into components in the magnetic meridian plane (meridional) and perpendicular (zonal) to the magnetic meridian. Here we discuss only the characteristics of the meridional (vertical) ion drift. Shown in Figures 1–8 are the median values of the drifts denoted by asterisks along with the average absolute deviation from the median for all points. The total ion density is a solid gray line in the lower section of each panel, shown without a variance for clarity. Also shown in the upper section of each panel (green line) is the average fractional contribution of O+ to the total ion concentration. The red horizontal line shows the mean drift over all local times for each longitude sector. The points are asymmetrically distributed in magnetic latitude since the satellite has a 13° inclination and the magnetic equator lies alternately at 10° north or south of the equator depending on the longitude.

[12] Figures 1–8 shows the local time variations in the meridional ion drift, total ion concentration and O+ fraction for different longitude regions from winter 2008 through 2010. The mean solar flux and standard deviation for each season is listed in Table 1. For comparison, drifts from the Scherliess-Fejer (SF) model [*Scherliess and Fejer*, 1999] contained within the International Reference Ionosphere (IRI) [*Bilitza and Reinisch*, 2008] over the same day range and solar flux levels are presented in blue. In general, this comparison highlights the presence of a semidiurnal component in measured ion drifts, characterized by downward

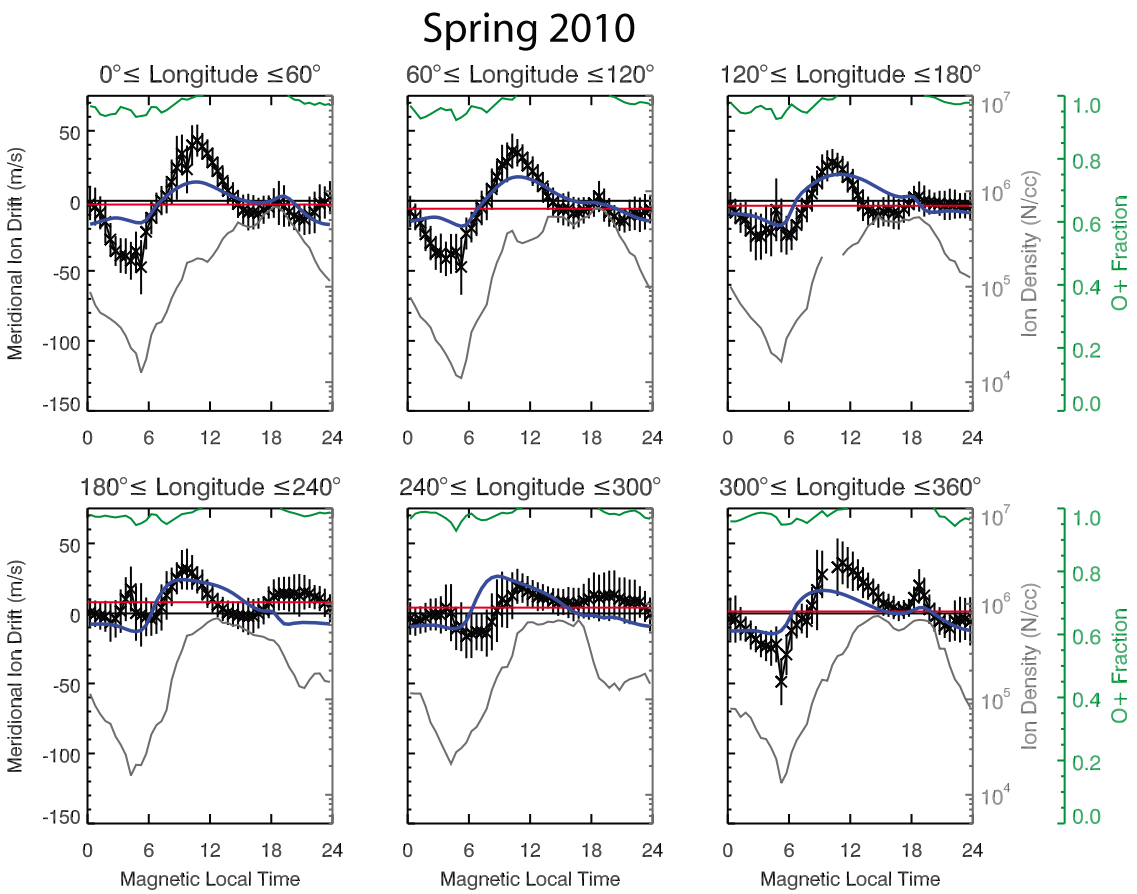

Figure 4. Magnetic local time variations in the meridional ion drift, total ion concentration, and O+ fraction for different longitude regions during spring 2010. Drifts from the Scherliess-Fejer model are included in blue.

drift perturbations in the early afternoon and upward drift perturbations during the night.

[13] Downward afternoon drifts are observed in all seasons presented here and are observed over all longitudes, though downward drifts may not be present at all longitudes in a particular season. Downward afternoon drifts are strongest during both the June and December solstices, in particular during the 2009 season (Figures 6 and 7), reaching magnitudes greater than 20 m s^{-1}.

[14] Compared to expectations of downward drifts through the night there is an upward perturbation in meridional drifts. Upward drifts with medians of 20 m s^{-1} or more across midnight are observed between 180°–240° during winter 2008/2009 (Figure 5) and between 0°–120° during summer 2009 (Figure 7). The upward perturbation in drifts at night can be seen in all longitudes and seasons, though not necessarily all longitudes in a particular season. Though ion drifts may still be downward at night, as seen between 0°–120° during fall 2009 (Figure 1), the magnitude of the downward drifts is minimized near midnight. Upward drifts after midnight are observed in regions of positive declination, in particular during the equinox seasons. Stronger upward drifts are observed with the increase in solar flux from equinox 2009 (Figures 1 and 3) to 2010 (Figures 2 and 4) between 180°–240°. During spring 2009 (Figure 3), drifts between 60°–120° are generally like expectations illustrated by the SF model, upward drifts during the day and downward at night, though some differences remain. During spring 2010 (Figure 4), weakly downward afternoon drifts are observed along with a minimum in downward drifts across midnight, demonstrating an increased semidiurnal component compared to the previous spring. Thus the presence of the semidiurnal driver in measurements varies both in time and in space.

[15] The local time distribution of the average ion density is generally in accord with the local time distribution of the drifts. For example in Figure 1, the ion density peaks a little after local noon following the rapid decline in the upward drift. The decline is interrupted near 18:00 MLT by a small increase in density produced by the postsunset enhancement, but otherwise continues to decrease to reach a minimum just before sunrise. The minimum density is strongly correlated with the time integral of the downward drift and thus the lowest presunrise density is observed in the longitude regions 300°–120° where downward drifts prevail through most of the night. Variations in the O+ fraction are also consistent with local time variations in the ion drift. The percentage of oxygen falls after sunset, decreasing through the night. The lowest oxygen concentrations at dawn are the result of a contracted atmosphere because of the extended solar minimum [*Heelis et al.*, 2009]. Oxygen concentrations rise rapidly after sunrise, peaking above 95% oxygen after noon.

[16] In particular, the local time variation in the ion density in Figure 6 supports the deviations in meridional drifts from the SF model. Between 180° and 300° the ion density is

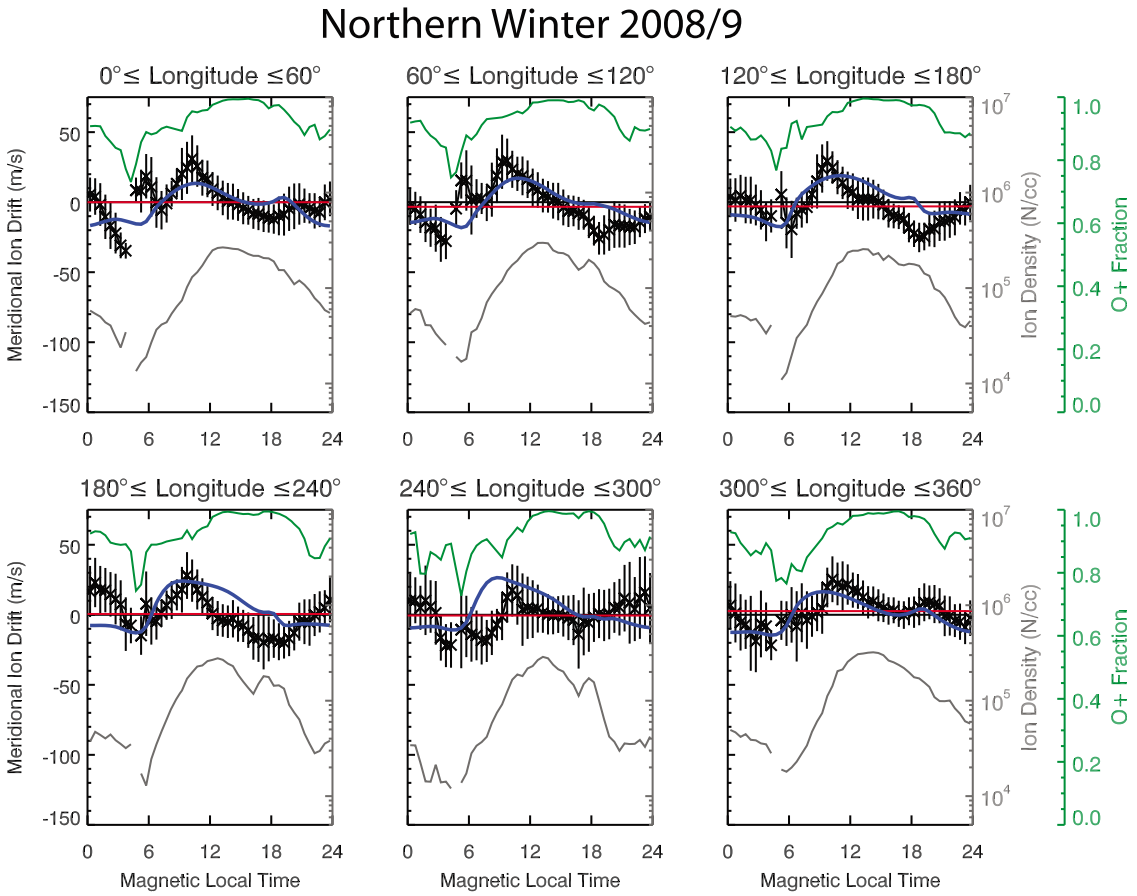

Figure 5. Magnetic local time variations in the meridional ion drift, total ion concentration, and O+ fraction for different longitude regions during northern winter, December 2008 to January 2009. Drifts from the Scherliess-Fejer model are included in blue.

depressed in the region near 14:00 local time when the ion drift becomes significantly downward. Upward drifts at night reduce the rate of plasma density decay and the largest dawn densities for the season are also observed in this sector.

[17] The increase in solar flux for fall 2010 (Figure 2) compared to the previous fall (Figure 1) results in significantly increased ion densities at a given altitude. Peak daytime densities double from 2009 to 2010, while minima in the midnight to predawn period increase by almost an order of magnitude. The increase in solar activity is also reflected in the fraction of O+ ions at the satellite altitude. Concentrations are above 95% at all local times during 2010 compared to dawn minima of 85% in 2009.

[18] Peak downward drifts are found before dawn with magnitudes approaching 50 m s^{-1} during spring 2010 (Figure 4). Large downward drifts are also observed during all presented solstices though the presence of photoemission within the instrument combined with the low densities before dawn limit measurements in this area.

[19] As illustrated by the SF model, a weak postsunset enhancement is expected because of the low levels of solar activity. Drifts similar to these predictions are observed in spring 2009 (Figure 3), drifts are near zero across sunset transitioning downward through the night. Weak enhancements are observed in the fall and spring of 2009 (Figures 1 and 3) that increase as expected with F10.7 levels in 2010 (Figures 2 and 4).

[20] The presented absolute deviations from the median meridional drifts reflect the day-to-day variability of the ionosphere [*Fejer et al.*, 2008] as well as longitudinal gradients in the meridional drift [*Araujo-Pradere et al.*, 2011]. Thus, on a given day and at a particular longitude, meridional drifts can depart from the median values presented here, in some cases by more than 10 m s^{-1}. Nighttime measurements tend to display larger variations because of the presence of irregularities.

3. Validation

[21] The precession of the C/NOFS orbit and the restrictions placed on the altitude for high-quality data from the CINDI instrument provide only limited opportunities to compare the instrument measurements with the same parameter derived from the Jicamarca radar. While a more exhaustive comparison is forthcoming (B. G. Fejer and E. Pacheco, private communication, 2010), Figure 9 provides a comparison made in 2009 and 2010 during nighttime and daytime passes of the C/NOFS satellite within 30° longitude of Jicamarca and 5° of the magnetic equator. Jicamarca measurements are averaged vertical drifts for the 247 km altitude

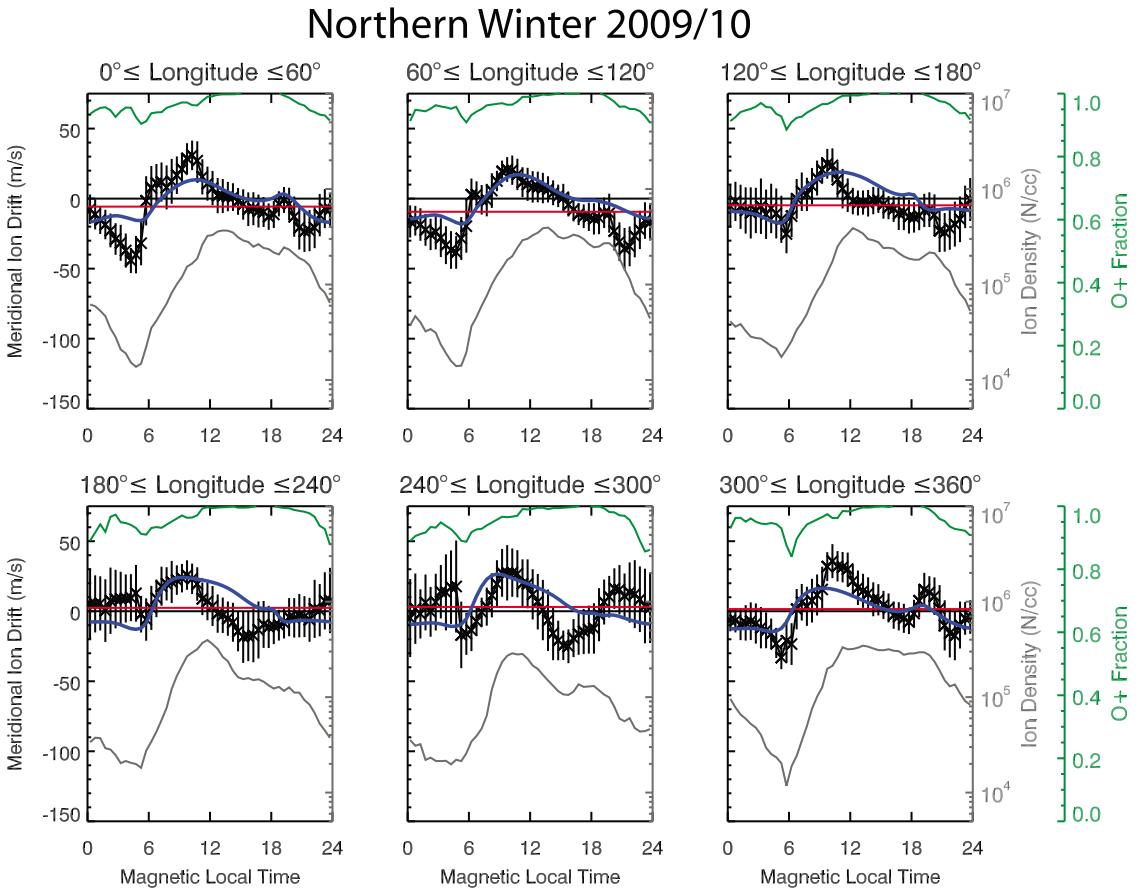

Figure 6. Magnetic local time variations in the meridional ion drift, total ion concentration, and O+ fraction for different longitude regions during northern winter, December 2009 to January 2010. Drifts from the Scherliess-Fejer model are included in blue.

range with a 60 km average and a measurement error less than 5 m s^{-1}. The comparisons are very encouraging.

[22] During the nighttime the signal-to-noise ratio is quite small because of the low ionospheric density and the high degree of geophysical variability. Nevertheless the major features in each data set are the same and the deviations between them are well below the variability seen in the IVM data and specified by the scatter bars attached to each point. During the daytime the confidence levels in the Jicamarca data are much higher than those during the night. Again the local time variations show a great deal of variability but the agreement between the two data sets provides a great deal of confidence in the methodology that we have employed to extract the vertical drift from the CINDI data. Since the IDM calibration is not longitude specific, the agreement with Jicamarca supports measurements in other regions. Excellent agreement between CINDI and Jicmamarca was also reported by *Rodrigues et al.* [2011] during a sudden stratospheric warming event.

4. Discussion

[23] The data presented in this paper were taken during a prolonged period of low solar activity when the average F10.7 was between 68 and 80 solar flux units (1 sfu = 10^{-22} W m^{-2} Hz^{-1}). Thus the results are not immediately comparable to other satellite measurements from Atmosphere Explorer [*Fejer et al.*, 1995] or from ROCSAT 1 [*Fejer et al.*, 2008]. The average patterns of vertical ion drift described here have some important variances from the statistical data gathered from the Jicamarca radar [*Fejer et al.*, 1979, 1991]. However, there are some features that appear in previously reported observations. For example, during the daytime the data shown here and that obtained from the Jicamarca radar agree that the region of upward drift is largely confined to the period before local noon. After local noon the drifts are very weak and may be upward or downward. Measurements by C/NOFS show that in the afternoon sector the vertical drift is generally very weak and can be substantially downward in different longitude regions and different seasons. Downward drifts are seen in the 180°–300° longitude sector in northern winter seasons and the 300°–120° longitude sector in the northern summer and fall seasons. This variation may be due in part to a seasonal variation in the influence of a semidiurnal tide in the E region. The semidiurnal drift component may also be significant during the night, being responsible for upward drifts near midnight. The influence of the semidiurnal tide at middle latitudes is well documented [*Fesen et al.*, 1991] but during this solar minimum period our results suggest that it is equally important close to the magnetic equator. It appears at all seasons and is easily identified by the

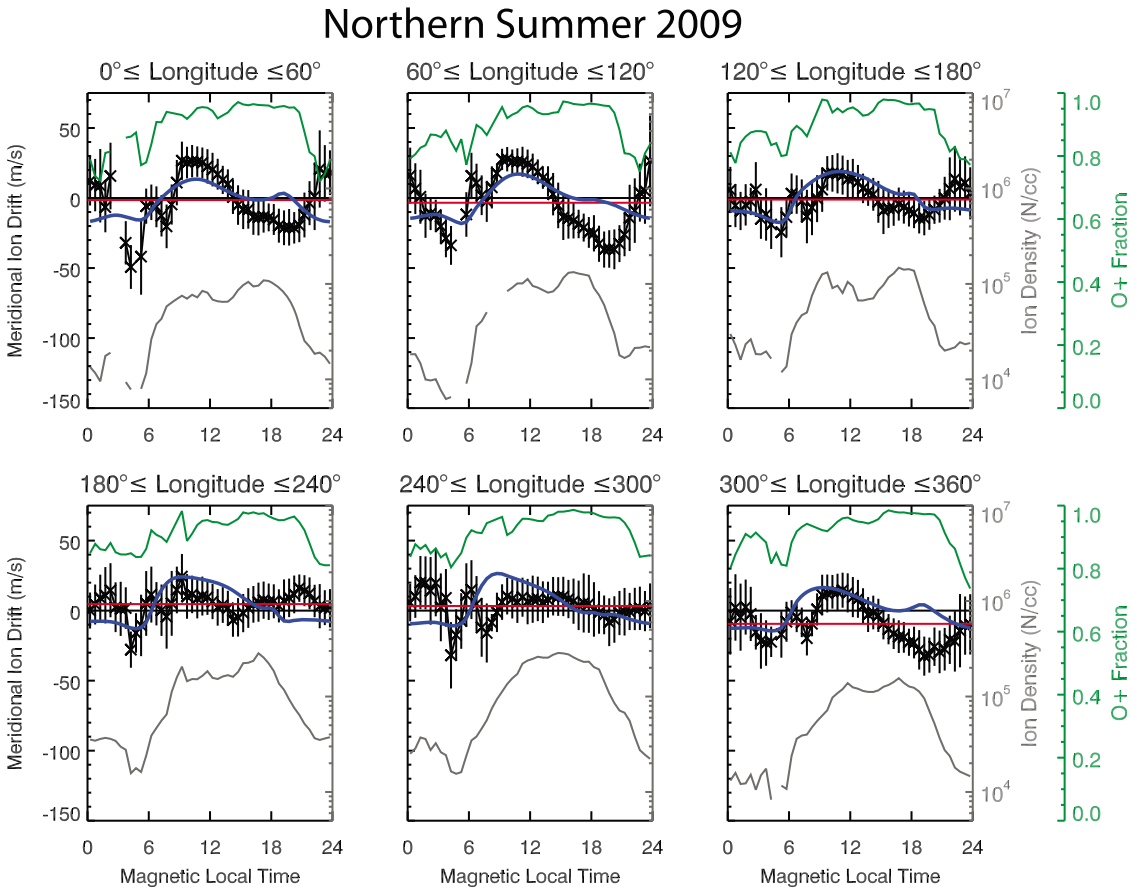

Figure 7. Magnetic local time variations in the meridional ion drift, total ion concentration, and O+ fraction for different longitude regions during northern summer, June–July 2009. Drifts from the Scherliess-Fejer model are included in blue.

strongest vertical drifts in the period before local noon and weak or downward drifts in the afternoon.

[24] Additional support for the presence of a semidiurnal tide is found through comparison to drifts observed by *Fejer* [1993] over Arecibo, located within the 240°–300° sector. For F10.7 levels near 80, peaks in upward drift are observed near 02:00–04:00 and 10:00–12:00 MLT. Downward drifts near dawn separate these peaks and the drift becomes downward after noon, with a weak postsunset enhancement. The same drift pattern is observed by CINDI in regions of positive declination for seasons with a F10.7 near 80 (Figures 2, 4, and 6). As expected, CINDI observes a larger postsunset enhancement at lower apex heights than is observed at Arecibo. We note that the postsunset enhancement is largely absent for solar flux levels less than 80. This dependence on the solar flux is also seen at Jicamarca [*Fejer et al.*, 1991] but the relative influence of the winds and conductivity on this behavior is yet to be understood.

[25] The largest downward drifts are seen at all longitudes and all seasons in the postmidnight sector. They are most prominent in the 300° to 120° longitude sector during all seasons. In this presunrise region the downward drifts are quite variable but the median drift can be substantial, sometimes exceeding 50 m s^{-1}. In this same region the total ion number density in the topside near 450 km altitude shows a local minimum below 10^4 cm^{-3} and a local minimum in the relative O+ concentration. *Huang et al.* [2009] have described the details of this presunrise density feature which are consistent with the observed downward drifts.

[26] Downward drifts that peak in the presunrise period are a feature that appears in much of the past literature. In particular *Pacheco et al.* [2010] indicate such downward drifts are seen in the ROCSAT 1 data during solar maximum. They are most prominent during northern summer in the African and Indian sectors, consistent with observations here. The measurements are taken at altitudes above 400 km, well above the *F* peak altitude. Thus the deep density minimum that accompanies the drifts is produced by the downward drift and is accompanied as expected by a decrease in the relative concentration of O+.

[27] Significant upward drifts have been observed near midnight in the northern summer and winter seasons of 2009, coincident with the observation of significant postmidnight irregularities. Here we briefly discuss the consistency of the drift patterns described above and the irregularity occurrence described by *Heelis et al.* [2010]. For northern summer 2009 (Figure 7), downward drifts after sunset are prevalent and will effectively suppress the growth of irregularities. However, the greatest occurrence of irregularities is found between 330° and 120° after midnight and in this region the vertical drift turns sharply upward to reach peak velocities of 20 m s^{-1}. The earliest onset of irregularities is found near

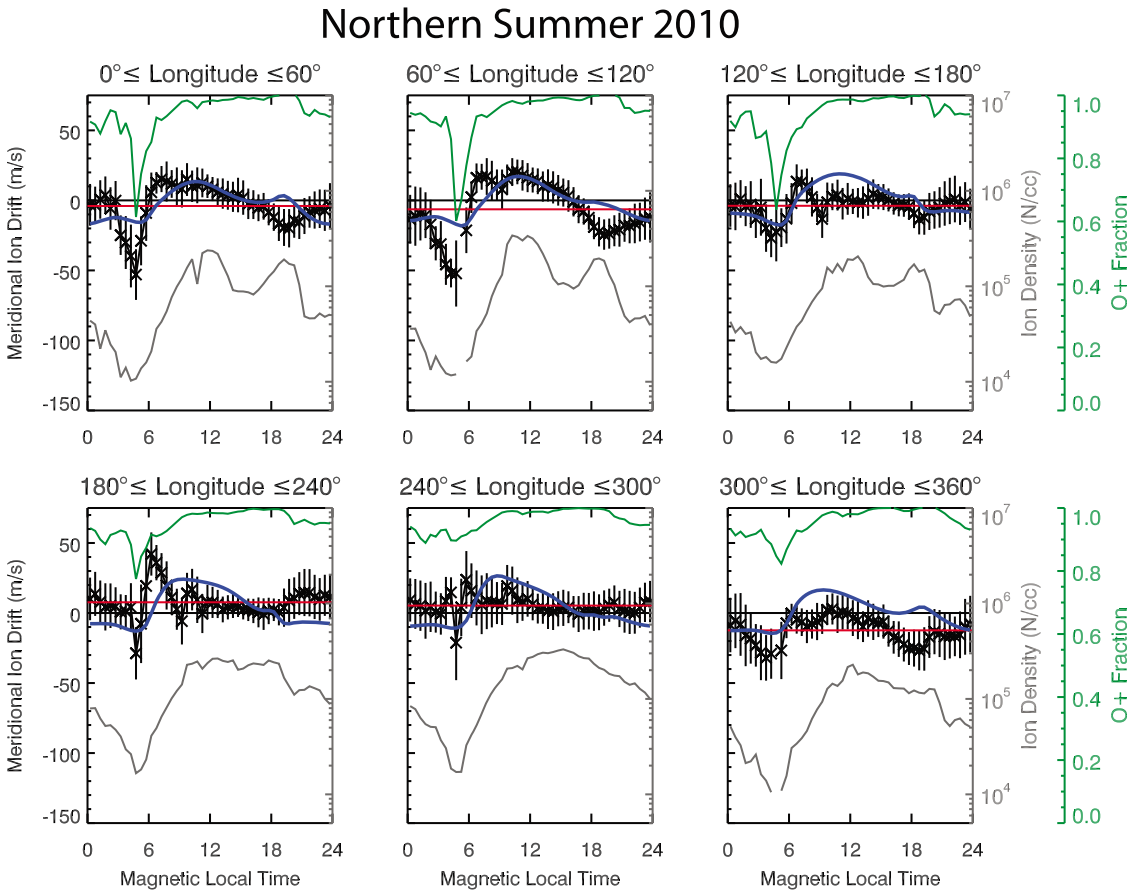

Figure 8. Magnetic local time variations in the meridional ion drift, total ion concentration, and O+ fraction for different longitude regions during northern summer, June–July 2010. Drifts from the Scherliess-Fejer model are included in blue.

180° consistent with the early onset of upward drifts in the same sector. A minimum in the occurrence of irregularities is located between 240°–300° longitude, a sector with drifts near zero after sunset and into midnight. After midnight, upward drifts are present though significant ion density irregularities are not observed.

[28] For the northern winter 2009 season, the maximum occurrence of irregularities was found between 180° and 270° longitude. In the 180° to 240° sector of Figure 5 downward drifts of -20 m s^{-1} at sunset transition to upward drifts across midnight with a peak near 20 m s^{-1}. The 240°–300° sector has upward drifts after sunset and through midnight with corresponding irregularities that begin near 2100 local time. A postsunset enhancement with upward drifts near 10 m s^{-1} is found between 300° and 360°, a region characterized by a maximum in irregularities premidnight. A minimum in occurrence of irregularities is observed between 60° and 120° where drifts are downward through the night.

[29] The correlation of drifts and irregularities is consistent with previous observations at Jicamarca [*Fejer et al.*, 1999] where it was concluded that postmidnight irregularities required upward drifts preceded by downward drifts. The observed preponderance of postmidnight irregularities during the 2009 season [*Heelis et al.*, 2010] reflects the weakness/absence of post sunset enhancements and the presence of upward drifts near midnight presented here.

[30] Ignoring the influence of external drivers from the magnetosphere and solar wind, the *F* region equatorial drifts result largely from polarization fields established in the daytime from *E* region winds and polarization fields established during the nighttime by *F* region winds. It is customary to assume that the daytime *E* region conductance is much larger than the *F* region conductance and that any currents driven by *F* region winds during the daytime can be closed through the E region with a negligible electric field. Further, we assume that the daytime *E* region conductance is uniform and thus only the presence of an *E* region wind variation can account for the observed daytime variation in observed

Table 1. Solar F10.7 Mean Values and Standard Deviations as a Function of Season[a]

	Mean	Standard Deviation
Winter 2008/2009	69.4	0.9
Spring 2009	69.7	0.9
Summer 2009	69.9	1.7
Fall 2009	78.3	2.2
Winter 2009/2010	80.8	5.4
Spring 2010	74.7	4.6
Summer 2010	79.6	4.6
Fall 2010	82.9	4.7

[a]Values listed in solar flux units (1 sfu = 10^{-22} W m^{-2} Hz^{-1}).

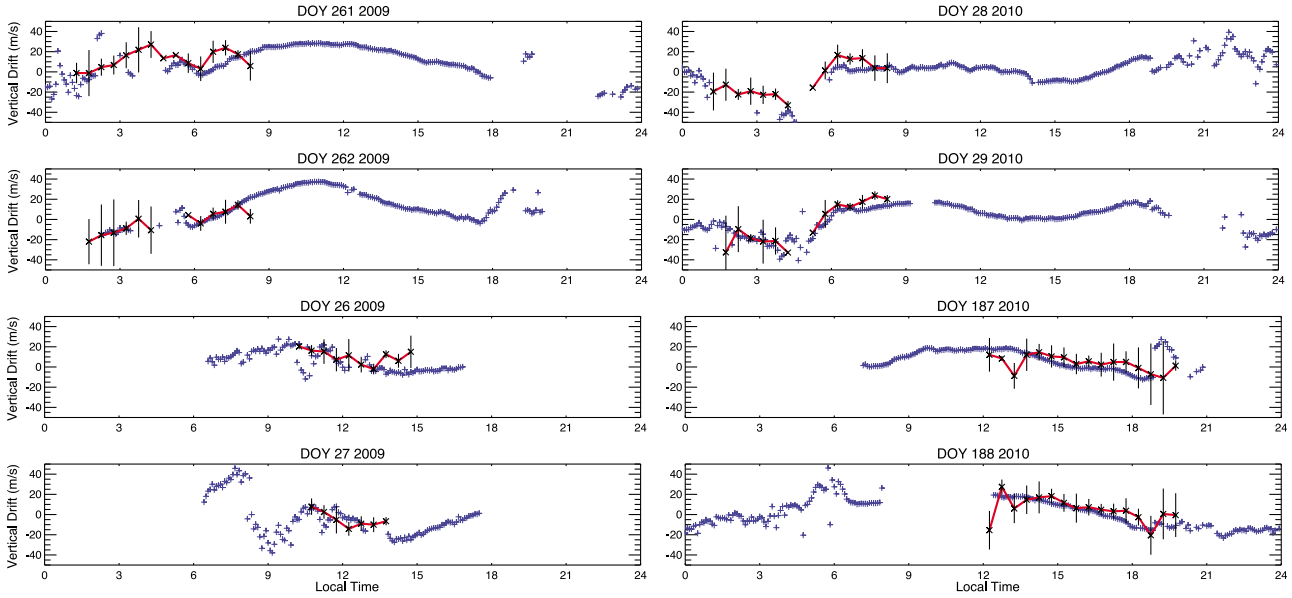

Figure 9. Comparison of vertical ion drifts measured by the Communication/Navigation Outage Forecast System (C/NOFS) (red) and Jicamarca (blue) where C/NOFS measurements are restricted to areas within 30° longitude of Jicamarca and 5° of the magnetic equator.

E × **B** drifts. A semidiurnal tide in the *E* region will act to enhance the prenoon drift, to increase the local time gradient in the drift across sunrise and to suppress or even reverse the afternoon drift imposed by a dawn-to-dusk electric field. If zonal *F* region winds are in phase with the semidiurnal tide during the day then downward afternoon drifts imply upward drifts near midnight. A meridional (northward) semidiurnal wind component is also expected that typically exhibits a phase difference of several hours compared to zonal winds [*Fesen et al.*, 1991]. These meridional winds may be responsible for upward drifts after midnight in regions with significant magnetic declination. The influence of meridional (northward) winds on vertical drifts as a function of magnetic declination has been reported by *Hartman and Heelis* [2007]. All these features are apparent in the average description of the vertical drift that we have provided. Recent observations of the vertical ion drift have shown that the semidiurnal component is amplified in the daytime during sudden stratospheric warming [*Chau et al.*, 2009; *Fejer et al.*, 2010]. Our results strongly suggest that in the period of low solar activity in 2009 and 2010, the presence of a semidiurnal tide is a pervasive feature of the observed drift pattern at the magnetic equator at all times.

[31] It may also be prudent to consider the influence of *F* region winds even during the daytime. At night the influence of the *F* region winds is invoked to explain the appearance of the so-called prereversal drift enhancement [*Eccles*, 1998] and to explain the enhanced downward drifts seen in the presunrise sector [*Pacheco et al.*, 2010]. However, the differences in the E region and F region conductance during the daytime may not be so large that local time variations in the zonal *F* region wind can be neglected. Though F region densities may not be as large as the E region, the longer path length of field lines through the F region can lead to a larger flux tube integrated conductivity. When the ratio of integrated F and E region Pedersen conductivities is near unity or greater, F region dynamo behavior will predominate [*Crain et al.*, 1993]. Recent modeling of electric fields using different versions of a wind model [*Huba et al.*, 2010] reveals radical differences in the **E** × **B** drift patterns during the daytime and nighttime. While an analysis of the wind patterns in the E and *F* regions has not been completed, it is evident that our lack of knowledge of the wind is a significant barrier to completing the interpretation of the observed ion drifts.

5. Conclusions

[32] We have described the local time distribution of meridional (vertical) drifts observed by the CINDI sensors on the C/NOFS spacecraft during the prolonged solar minimum that includes data from late 2008 through 2010. The meridional drifts depart significantly from the usual expectation of an approximate sinusoidal variation with upward drifts by day and downward drifts by night. During the afternoon drifts are very weak and can sometimes be downward. Likewise across the midnight sector the drifts are very weak and may sometimes be upward. The deviations in the expected behavior of the drift are attributed to an increased role played by a semidiurnal tide in the equatorial region. The behavior of the total ion density is consistent with the average behavior of the ion drift for which the absence of large upward drifts during the day or a prereversal enhancement leads to very low topside ion densities in the predawn sector. The presence of downward drifts across sunset and upward drifts across midnight is also consistent with the delay in the appearance of ionospheric irregularities to the postmidnight sector. A comparison between CINDI and Jicamarca Radio Observatory shows good agreement, supporting the methodology used to extract and construct the meridional drifts from CINDI measurements. In accordance with previous observations, a prereversal enhancement is small or absent near dusk

at the lowest solar activity levels in 2009 but becomes more clearly identifiable for mean F10.7 levels above 80. The appearance of a weak postsunset drift enhancement suggests that the *F* region dynamo is still an active contributor to the observed ion drift pattern but the relative importance of the *F* region winds and *F* region conductance cannot be assessed at this time.

[33] **Acknowledgments.** This work is supported at the University of Texas at Dallas by NASA grant NNX10AM94G. The C/NOFS mission is supported by the Air Force Research Laboratory, the Department of Defense Space Test Program, the National Aeronautics and Space Administration (NASA), the Naval Research Laboratory, and the Aerospace Corporation. The Jicamarca Radio Observatory is a facility of the Instituto Geofisico del Peru operated with support from the NSF AGS-0905448 through Cornell University. Jicamarca data was obtained using the Madrigal database.

[34] Robert Lysak thanks Fabiano Rodrigues and the other reviewers for their assistance in evaluating this paper.

References

Anderson, D., and E. A. Araujo-Pradere (2010), Sudden stratospheric warming event signatures in daytime **E** × **B** drift velocities in the Peruvian and Philippine longitude sectors for January 2003 and 2004, *J. Geophys. Res.*, *115*, A00G05, doi:10.1029/2010JA015337.

Araujo-Pradere, E. A., D. Anderson, M. Fedrizzi, and R. Stoneback (2011), Communications/Navigation Outage Forecasting System observational support for the equatorial **E** × **B** drift velocities associated with the four-cell tidal structures, *Radio Sci.*, *46*, RS0D09, doi:10.1029/2010RS004557.

Bilitza, D., and B. W. Reinisch (2008), International Reference Ionosphere 2007: Improvements and new parameters, *Adv. Space Res.*, *42*, 599–609, doi:10.1016/j.asr.2007.07.048.

Blanc, M., and A. D. Richmond (1980), The ionospheric disturbance dynamo, *J. Geophys. Res.*, *85*(A4), 1669–1686, doi:10.1029/JA085iA04p01669.

Chau, J. L., B. G. Fejer, and L. P. Goncharenko (2009), Quiet variability of equatorial **E** × **B** drifts during a sudden stratospheric warming event, *Geophys. Res. Lett.*, *36*, L05101, doi:10.1029/2008GL036785.

Crain, D., R. Heelis, and G. Bailey (1993), Effects of electrical coupling on equatorial ionospheric plasma motions: When is the *F* region a dominant driver in the low-latitude dynamo?, *J. Geophys. Res.*, *98*(A4), 6033–6037, doi:10.1029/92JA02195.

Eccles, J. (1998), Modeling investigation of the evening prereversal enhancement of the zonal electric field in the equatorial ionosphere, *J. Geophys. Res.*, *103*(A11), 26,709–26,719, doi:10.1029/98JA02656.

Fejer, B. (1993), *F* region plasma drifts over Arecibo: Solar cycle, seasonal, and magnetic activity effects, *J. Geophys. Res.*, *98*(A8), 13,645–13,652, doi:10.1029/93JA00953.

Fejer, B., D. Farley, and R. Woodman (1979), Dependence of equatorial *F* region vertical drifts on season and solar cycle, *J. Geophys. Res.*, *84*(A10), 5792–5796, doi:10.1029/JA084iA10p05792.

Fejer, B., S. Gonzalez, E. de Paula, and R. Woodman (1991), Average vertical and zonal *F* region plasma drifts over Jicamarca, *J. Geophys. Res.*, *96*(A8), 13,901–13,906, doi:10.1029/91JA01171.

Fejer, B., E. de Paula, and R. Heelis (1995), Global equatorial ionospheric vertical plasma drifts measured by the AE-E satellite, *J. Geophys. Res.*, *100*(A4), 5769–5776, doi:10.1029/94JA03240.

Fejer, B., L. Scherliess, and E. de Paula (1999), Effects of the vertical plasma drift velocity on the generation and evolution of equatorial spread *F*, *J. Geophys. Res.*, *104*, 19,859–19,869.

Fejer, B., J. Jensen, and S.-Y. Su (2008), Quiet time equatorial *F* region vertical plasma drift model derived from ROCSAT-1 observations, *J. Geophys. Res.*, *113*, A05304, doi:10.1029/2007JA012801.

Fejer, B. G., M. E. Olson, J. L. Chau, C. Stolle, H. Lühr, L. P. Goncharenko, K. Yumoto, and T. Nagatsuma (2010), Lunar-dependent equatorial ionospheric electrodynamic effects during sudden stratospheric warmings, *J. Geophys. Res.*, *115*, A00G03, doi:10.1029/2010JA015273.

Fesen, C., R. Roble, and E. Ridley (1991), Themospheric tides at equinox: Simulations with coupled composition and auroral forcings, 2. Semidiurnal component, *J. Geophys. Res.*, *96*(A3), 3663–3677, doi:10.1029/90JA02189.

Hagan, M., A. Maute, R. Roble, A. Richmond, T. Immel, and S. England (2007), Connections between deep tropical clouds and the Earth's ionosphere, *Geophys. Res. Lett.*, *34*, L20109, doi:10.1029/2007GL030142.

Hartman, W. A., and R. A. Heelis (2007), Longitudinal variations in the equatorial vertical drift in the topside ionosphere, *J. Geophys. Res.*, *112*, A03305, doi:10.1029/2006JA011773.

Heelis, R. A., and W. B. Hanson (1998), Measurements of thermal ion drift velocity and temperature using planar sensors, in *Measurement Techniques in Space Plasmas: Particles*, *Geophys. Monogr. Ser.*, vol. 102, edited by F. Pfaff, E. Borovsky, and T. Young, pp. 61–71, AGU, Washington, D. C., doi:10.1029/GM102p0061.

Heelis, R. A., W. R. Coley, A. G. Burrell, M. R. Hairston, G. D. Earle, M. D. Perdue, R. A. Power, L. L. Harmon, B. J. Holt, and C. R. Lippincott (2009), Behavior of the O+/H+ transition height during the extreme solar minimum of 2008, *Geophys. Res. Lett.*, *36*, L00C03, doi:10.1029/2009GL038652.

Heelis, R. A., R. Stoneback, G. D. Earle, R. A. Haaser, and M. A. Abdu (2010), Medium-scale equatorial plasma irregularities observed by Coupled Ion-Neutral Dynamics Investigation sensors aboard the Communication Navigation Outage Forecast System in a prolonged solar minimum, *J. Geophys. Res.*, *115*, A10321, doi:10.1029/2010JA015596.

Huang, C. Y., F. A. Marcos, P. A. Roddy, M. R. Hairston, W. R. Coley, C. Roth, S. Bruinsma, and D. E. Hunton (2009), Broad plasma decreases in the equatorial ionosphere, *Geophys. Res. Lett.*, *36*, L00C04, doi:10.1029/2009GL039423.

Huba, J., G. Joyce, and J. A. Fedder (2000), Sami2 is Another Model of the Ionosphere (SAMI2): A new low-latitude ionosphere model, *J. Geophys. Res.*, *105*(A10), 23,035–23,053, doi:10.1029/2000JA000035.

Huba, J. D., G. Joyce, J. Krall, C. Siefring, and P. A. Bernhardt (2010), Self-consistent modeling of equatorial dawn density depletions with SAMI3, *Geophys. Res. Lett.*, *37*, L03104, doi:10.1029/2009GL041492.

Kil, H., S. Oh, L. Paxton, and T. Fang (2009), High-resolution vertical **E** × **B** drift model derived from ROCSAT-1 data, *J. Geophys. Res.*, *114*(A10), A10314, doi:10.1029/2009JA014324.

Millward, G., I. Müller-Wodarg, and A. Aylward (2001), An investigation into the influence of tidal forcing on *F* region equatorial vertical ion drift using a global ionosphere-thermosphere model with coupled electrodynamics, *J. Geophys. Res.*, *106*(A11), 24,733–24,744, doi:10.1029/2000JA000342.

Pacheco, E. E., R. A. Heelis, and S. Y. Su (2010), Quiet time meridional (vertical) ion drifts at low and middle latitudes observed by ROCSAT-1, *J. Geophys. Res.*, *115*, A09308, doi:10.1029/2009JA015108.

Peymirat, C., A. D. Richmond, and A. T. Kobea (2000), Electrodynamic coupling of high and low latitudes: Simulations of shielding/overshielding effects, *J. Geophys. Res.*, *105*(A10), 22,991–23,003, doi:10.1029/2000JA000057.

Rodrigues, F. S., G. Crowley, S. M. I. Azeem, and R. A. Heelis (2011), C/NOFS detection of the equatorial ionospheric electric field response to the 2009 major sudden stratospheric warming event, *J. Geophys. Res.*, *116*, A09316, doi:10.1029/2011JA016660.

Scherliess, L., and B. G. Fejer (1999), Radar and satellite global equatorial *F* region vertical drift model, *J. Geophys. Res.*, *104*(A4), 6829–6842, doi:10.1029/1999JA900025.

A. G. Burrell, W. R. Coley, R. A. Heelis, and R. A. Stoneback, Physics Department, Hanson Center for Space Sciences, University of Texas at Dallas, MS/WT15, PO Box 830688, Richardson, TX 75080, USA. (rstoneba@utdallas.edu)

B. G. Fejer and E. Pacheco, Center of Atmospheric and Space Sciences, Utah State University, 4405 Old Main Hill, Logan, UT 84332, USA.